CrossMark

sciendo Applied Mathematics and Nonlinear Sciences 3(2) (2018) 553–570

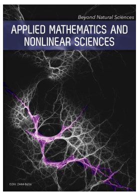

Applied Mathematics and Nonlinear Sciences

https://www.sciendo.com

Designing optimal trajectories for a skimmer ship to clean, recover and prevent the oil spilled on the sea from reaching the coast

Susana Gomez[(a)], Benjamin Ivorra[(b)] †, Angel M. Ramos[(b)].

[(a)] Instituto de Matemáticas Aplicadas y Sistemas,

Universidad Nacional A. de México. México.

[(b)] Departamento de Análisis Matemático y Matemática Aplicada,

Instituto de Matemática Interdisciplinar,

Universidad Complutense de Madrid. España.

Submission Info

Communicated by Juan L.G. Guirao
Received 18th September 2018
Accepted 18th December 2018
Available online 31st December 2018

Abstract

In this work, we use an Eulerian mathematical model to forecast the movement of oil spills in the open sea and we design objective functions to obtain optimal trajectories for skimmer ships to clean and recover the oil. Here, we first validate the ability of this mathematical model to forecast the fate of the oil by comparing our results with satellite images. Then, we create a synthetic study case based on real data, and we show that following optimal trajectories greatly improves the amount of oil recovered at the whole area of study.

Keywords: Forecast the evolution of oil spills; Eulerian mathematical model; Optimal trajectories for skimmer ships; Avoid the oil reaching the coast; Clean and recover oil spills.
AMS 2010 codes: 46N10;34A34; 35Qxx.

1 Introduction

Oil spill contamination in the open sea has produced some of the worst environmental disasters in history [6,22]. In the case of the Prestige accident (Galicia, Spain 2002), more than 10 million gallons of heavy/residual fuel oil were spilled [27] and thousands of kilometers of coastline in Spain, France and Portugal were polluted [5]. This spill is considered as the largest environmental disaster in the history of both Spain and Portugal, and the cost of the disaster was evaluated to be more than 770 million euros [20]. Because of its large geographical spread, the spill reached all types of marine habitat, from offshore depths to shallow creeks. The worst affected

†Corresponding author.
Email address: ivorra@mat.ucm.es

sciendo ISSN 2444-8656 doi:10.2478/AMNS.2018.2.00043 sciendo

habitats were in coastal areas, and this includes land damage caused by clean-up operations. Furthermore, this had economic repercussions on the inshore fishing and shellfish sector (e.g., [31]). The Prestige disaster was similar to that of the Exxon Valdez spill in terms of bird mortality, and it has been considered as one of the non-natural events most deadly to wildlife ever to have occurred in Europe. It was estimated that more than 50% of the sea birds and otters of the area were killed.

Another case is the ship 'Oleg Naydenov' that sunk near the Canary Islands coast, Spain, on 14 April , 2015 [16]. The tanks of this ship were filled with around 1400 tons of oil. The oil spilled into the sea with a flow estimated between 5 to 10 litres per hour. During several weeks, this oil spill provoked the pollution of the 'Gran Canaria' Island with several oil spots reaching its coastline.

One of the cleaning-recovering techniques for oil spills with light- to medium-viscosity oils, is the use of skimmer ships [7, 10]. These ships might use various pumps distributed along their waterline to suck the oil remaining at the surface of the water directly into storage units. These vessels move inside the oil spots to clean them as quickly as possible.

In order to be able to improve the efficiency of this pumping process, we first simulate the movement of the oil spots in both space and time using our Eulerian mathematical model proposed in [2, 16]. We note that in the literature, the prevailing models to forecast the fate oil spills on the sea are based on Lagrangian approaches [29,30]. However, in our case, we are considering in our model, additional effects related to the cleaning process, such as the transport and sink effects generated by the skimmer ships, which require to have a continuous (not particle wise) representation of the distribution of oil at each point of the considered area and at each time of the simulation. This explains why we have chosen an Eulerian approach. We then proceed to model the trajectory for a skimmer ship, and using a global optimisation algorithm, we optimize the trajectory to maximise the amount of oil pumped on a fixed period of time. Here, two scenarios are considered: cleaning on the whole area under study, or giving priority to prevent the oil from reaching the coast.

The technical ability of different pumps to suck several types of oil (from light to medium), have a large influence on the efficiency of the pumping process [15]. In this work, we present results comparing three types of pumps (considering only their pumping effective power), to show the advantage of creating optimal trajectories for the skimmers, independently of its pumping abilities. In particular, during the experiments proposed here, we consider the characteristics of the so called 'Controlled Floating Skimmer' pump, build by the Novetec company (see `http://www.novetec.es`), that may incorporate a crushing device in order to be able to pump emulsified oil (in this case, the pumping power is reduced). We have used the 2002 Prestige oil spill [16] as a test case, to show the efficiency of our approach. Although in the case of the Prestige spill, the use of Skimmer ships was not suited because of the high viscosity of the oil spilled, we are only using here, data from this hazard (i.e., the geographical region, the path and the amount of oil spilled, the wind and sea currents) to create a benchmark case.

We also highlight the fact that the proposed methodology may be applied to any other cleaning method requiring a trajectory planning.

The content of this article is as follows: In Section 2.1, we describe the main aspects of the Eulerian mathematical model we use to simulate the motion of the oil, taking into account the pumping process of a skimmer ship. In Section 2.2, we present the formulations of different objective functions to optimise the trajectory of the skimmer ship. In Section 3.1, we describe numerical experiments based on the 2016 Oleg Naydenov and the 2002 Prestige oil spills [16], citing the sources of data, to validate the forecast of the movement of the oil obtained with our model and to compare them with satellite images and discuss the results. Then, in Section 3.2, using the results obtained by the model, we solve several optimization problems to find optimal trajectories for the pumping process and analyse the behaviour of the solution regarding some key parameters (as the pumping power of the skimmer). Finally, some conclusions are made in Section 4

2 Materials and Methods

2.1 Eulerian Mathematical Model

Mathematical modelling of the transport and diffusion of an oil spill in the sea is of high interest to remediate the environmental impact (e.g., [24–26]).

We have developed an Eulerian model for the case where the density of the pollutant is smaller than that of one of the sea water (so that it remains at the surface) and assuming that the layer-thickness of the pollutant h, is known. We consider a 2D spatial domain of simulation (also called computational domain) $\Omega \subset \mathbb{R}^2$ large enough to ensure that the pollutant stays in the domain during the corresponding fixed simulation time interval $(0,T)$. We denote by $\partial\Omega_o$ the boundary of Ω in the open sea and by $\partial\Omega_c$ the boundary at the coast.

We denote by $c(x,t)$ the pollutant superficial concentration, measured as the amount of pollutant per surface area and time, at $\{x,t\} \in \Omega \times (0,T)$. We assume that the evolution of c is governed by a source of contaminant which is taken as a circle of radius R_s that follows a trajectory $\zeta \in C^1([0,T],\mathbb{R}^2)$ (that can be constant in the case of a fixed position polluted source, such as an offshore drilling rig) and spills an amount of oil $S(t)$ per unit of time. In addition, it is governed by the effect of the diffusion of the pollutant, the transport due to the wind and sea currents.

As we are interested in this work in studying the effect of a skimmer ship capable of pumping the spilled oil, the evolution of c is also affected by the transport and sink due to the pumping process. Furthermore, we assume that the skimmer ship follows a trajectory $\gamma \in C^1([0,T],\Omega)$.

From a practical point of view, a skimmer ship can be composed of multiple pumps, cleaning the water along the vessel waterline. However, for simplicity, we assume that there is only one pump, neglecting the length of the ship (small compared to the size of), which is a circle of radius R_p, pumping the fluid with velocity Q in the radial direction.

In order to avoid the undesired modelling effect of diffusion propagating at infinite speed [11], we use a non-linear diffusion term. We have also included a boundary condition with suitable absorbing properties to simulate the behaviour of the solution near the boundary of the computational domain.

For a detailed description of this model, see Reference [16].

The mathematical model follows:

$$\begin{cases} \dfrac{\partial c}{\partial t} - \nabla \cdot \dfrac{c^\kappa}{c_{\text{ref}}^\kappa}\mathbf{d}\nabla c + \nabla \cdot c\,\mathbf{o} + \nabla \cdot c\,\mathbf{p}_{\text{tol}} = -\dfrac{2Q}{R_p}\,c\;\chi_{B(\gamma(t),R_p)},\; \dfrac{S(t)}{2\pi R_S}\chi_{B(\zeta(t),R_s)}, & \text{in } \Omega \times (0,T), \\ L\dfrac{\partial c}{\partial t} + \left[-(\mathbf{o}+\mathbf{p}_{\text{tol}})c + \dfrac{c^\kappa}{c_{\text{ref}}^\kappa}\mathbf{d}\nabla c\right]\cdot \mathbf{n} = 0, & \text{on } \partial\Omega_o \times (0,T), \\ \left(\dfrac{c^\kappa}{c_{\text{ref}}^\kappa}\mathbf{d}\nabla c\right)\cdot \mathbf{n} = 0, & \text{on } \partial\Omega_c \times (0,T), \\ c(0) = c_0, \end{cases} \tag{1}$$

where:

- $B(a,b)$ is a ball of centre a and radius b.
- $\chi_{B(a,b)}(x) = \begin{cases} 0, \text{ if } x \in \Omega \backslash B(a,b), \\ 1, \text{ if } x \in B(a,b). \end{cases}$
- The function c_0 is the initial superficial concentration; we assume that c_0 has a compact support in Ω.
- $\mathbf{d} = \begin{pmatrix} d_1 & 0 \\ 0 & d_2 \end{pmatrix}$, d_1, d_2 (both >0) being the diffusion coefficients in the west-east and south-north directions.

- $\mathbf{o} = (o_1, o_2)$, where $o_i = s_i + w_i$ if sign$(o_1) \neq$sign(o_2), $o_i =$max$\{s_i, w_i\}$ if $s_i > 0$ and $w_i > 0$, $o_i =$min$\{s_i, w_i\}$ if $s_i < 0$ and $w_i < 0$. In the previous expression, $\mathbf{w} = (w_1, w_2)$ is the horizontal component of the wind velocity multiplied by a suitable drag factor and $\mathbf{s} = (s_1, s_2)$ is the surface current velocity of the sea. This term means that, for each direction in $\mathbb{R}^2$, the combined effects of the wind and sea velocities on the oil spots cannot be greater that the effect of the wind or sea alone.
- $\mathbf{p}_{\text{tol}}(\xi, t) = \max\left(\frac{\|\mathbf{p}(\xi,t)\|_2 - \text{tol}}{Q - \text{tol}}, 0\right) \cdot \mathbf{p}(\xi, t)$ is a corrected approximation of the velocity of the pump $\mathbf{p}(\xi, t) = QR_p \frac{\overrightarrow{\gamma(t)\xi}}{(\|\overrightarrow{\gamma(t)\xi}\|_2)^2}$, if $\xi \in \Omega \backslash B(\gamma(t), R_p)$, and 0, elsewhere [2]. This expression means that (i) the effect of the velocity field $\mathbf{p}$ on oil particles is neglected (i.e., $\mathbf{p}_{\text{tol}} = 0$) when $\|\mathbf{p}(\xi,t)\|_2 <$tol, for which the pump velocity is considered negligible regarding the diffusion coefficients; (ii) $\mathbf{p}_{\text{tol}}(\xi, t) = \mathbf{p}(\xi, t) = (0, 0)$, when $\|\overrightarrow{\gamma(t)\xi}\|_2 \leq R_p$; and (iii) $\|\mathbf{p}_{\text{tol}}(\xi,t)\|_2 < \|\mathbf{p}(\xi,t)\|_2$ and $\mathbf{p}_{\text{tol}}(\xi, t)$ is a smooth function when $\|\overrightarrow{\gamma(t)\xi}\|_2 > R_p$.
- c_{ref} is a reference pollutant concentration (here, $c_{\text{ref}} = 1$), and $\kappa > 0$ (typical values of κ being 1, 2 and 3).
- $L = \sqrt{(x_{\max} - x_{\min})^2 + (y_{\max} - y_{\min})^2}$ is the characteristic size (the diameter) of the domain Ω.

For the numerical solution of this equation, we use a finite volume discretization method coupled with an operator-splitting approach for the pumping term to reduce the computational time. Furthermore, to limit the artificial diffusion effect, typically produced by this kind of numerical model [11], we use second-order accurate time discretization schemes with nonlinear limiters to treat the transport. The full scheme of the considered numerical model can be found in Reference [16].

2.2 Design of Optimal Trajectories for a Cleaning Skimmer Ship

As mentioned in Section 1, we address the problem of finding an optimal trajectory for the skimmer ship, for a particular oil spill scenario during a fixed time interval $[0, T]$.

From a general point of view, we consider optimization problems of the form:

$$\min_{\gamma \in D_c} J_c(\gamma), \tag{2}$$

where $J_c(\gamma)$ is the objective function that is defined in the following, $D_c = \{\gamma \in C^1([0,T], \Omega)$ such that $|\gamma'(t)| \leq V_{\max}, \forall t \in [0,T]\}$ is the feasible region and $V_{\max}$ is the maximum speed of the ship when performing the pumping process. This restriction on the speed avoids to consider trajectories implying non-realistic ship velocities.

In this work, we have considered two particular optimisation problems associated with two different formulations of the objective function $J_c(.)$

- For the given time T, we minimize the concentration $c(\xi, T)$ of the remaining pollutant in the sea, which is equivalent to maximising the amount of pumped oil from the sea. In this case,

$$J_c(\gamma) = \int_0^T \Big(S(\tau) - c(\tau, \gamma(\tau))2\pi R_p Q\Big) \mathrm{d}\tau. \tag{3}$$

  where $\Big(S(\tau)$ is the amount of oil spilled per unit of time and $c(\tau, \gamma(\tau))2\pi R_p Q\Big)$ is the amount of pumped oil.

- For the given time T, we prioritise minimising the pollutant concentration that reaches the coast. To achieve this, we consider

$$J_c(\gamma) = \int_0^T \int_\Omega \text{coef}(x) c(\tau, x) \mathrm{d}x \mathrm{d}\tau, \tag{4}$$

where $\mathrm{coef}(x) = \lambda_1 \Big(1 - \big(\mathrm{dist}(x)/\max_{x\in\Omega}\mathrm{dist}(x)\big)\Big)^{\lambda_2} + \lambda_3$ is a weight function, with dist(x) being the distance between x and the nearest point to the coast (i.e., in the boundary $\partial\Omega_c$). λ_1, λ_2 and λ_3 are real parameters used to control the behaviour of coef(.). Function coef(.) gives more weight to the value of c for points near the coast than for points far from the coast.

These formulations take into consideration the evolution in time and space of the pollution concentration (obtained by solving the model), and specifically in the case of formulation (4), where the distances between the oil spots and the coast are variable.

In order to find numerically a smooth optimal pump trajectory (i.e., without sharp corners), we consider trajectories built by using cubic spline interpolation through $n_{\mathrm{npi}} \in$ 2-D interpolation points.

The set of interpolation points, denoted by P_{int}, is constructed by using a polar representation:

$$P_{\mathrm{int}} = \{(r_1,\theta_1),...,(r_{n_{\mathrm{npi}}},\theta_{n_{\mathrm{npi}}})\},$$

where $r_i \in [0, r_{\max}]$, with $r_{\max} = V_{\max}(T/n_{\mathrm{npi}})$ (modeling the ship velocity constraint), and $\theta_i \in [0,2\pi)$, for $i = 1,...,n_{\mathrm{npi}}$.

Given an interpolation point expressed in Cartesian coordinates $(x_k^{\mathrm{int}}, y_k^{\mathrm{int}})$, with $k \in \{1,...,n_{\mathrm{npi}}-1\}$, the next interpolation point $(x_{k+1}^{\mathrm{int}}, y_{k+1}^{\mathrm{int}})$ is built as:

$$x_{k+1}^{\mathrm{int}} = x_k^{\mathrm{int}} + r_k\cos(\theta_k),$$

$$y_{k+1}^{\mathrm{int}} = y_k^{\mathrm{int}} + r_k\sin(\theta_k).$$

The resulting interpolated trajectory is denoted by $\gamma_{(r_i,\theta_i)}$.

Furthermore, we need to avoid the ship leaving the domain of study Ω. To accomplish this, we project the trajectory $\gamma_{(r_i,\theta_i)}$ using an orthogonal projector on Ω.

Thus, the numerical optimization problem that we solve, is of the form:

$$\begin{array}{l} \qquad\qquad \min J(r_i,\theta_i) \\ \text{subject to} \\ \qquad 0 \le r_i \le r_{\max} \quad ,i = 1,...,n_{\mathrm{npi}}, \\ \qquad 0 \le \theta_i < 2\pi \quad ,i = 1,...,n_{\mathrm{npi}}, \end{array} \tag{5}$$

where $J(\{r_i,\theta_i\}_{i=1}^{\mathrm{npi}})$ is the considered version of the objective function $J_c(\gamma)$ and $\{(r_i,\theta_i)\}_{i=1}^{n_{\mathrm{npi}}} \subset D$ are the optimization variables (in this case, the coordinates of the trajectory of the skimmer ship) where $D = [0, r_{\max}] \times [0,2\pi)$ is the feasible region. The total number of optimization variables is $N = 2n_{\mathrm{npi}}$. Furthermore, if J_c is defined by formulation (3) then

$$J(\{r_i,\theta_i\}_{i=1}^{\mathrm{npi}}) = \int_0^T \Big(S(\tau) - c(\tau,\gamma_{(r_i,\theta_i)}(\tau))2\pi R_p Q\Big)\mathrm{d}\tau,$$

and if J_c is defined by formulation (4) then

$$J(\{r_i,\theta_i\}_{i=1}^{\mathrm{npi}}) = \int_0^T \int_\Omega \mathrm{coef}(x)c(\tau,x)\mathrm{d}x\mathrm{d}\tau.$$

A graphical representation of the function coef(.) is given in Figure 1.

Since Problem (5) exhibits many local minima [13], we need to use a global optimization method capable to find one global solution.

In order to solve optimisation Problem (2), we have developed an original hybrid global optimization method. This method is based on the combination of a particular Genetic Algorithm (GA) [12, 14, 28] and a

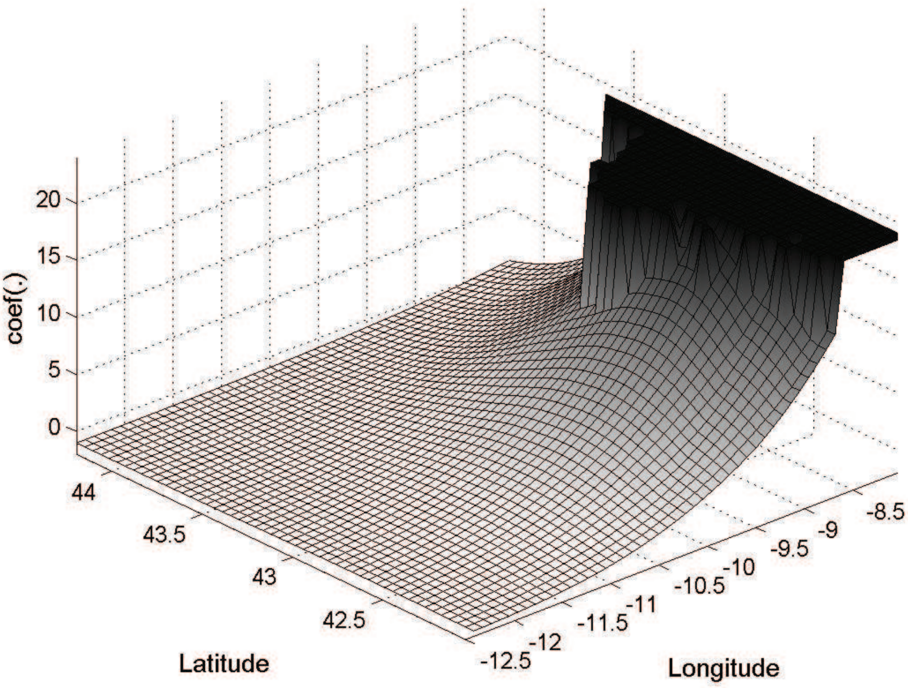

Fig. 1 Graphical representation of the function coef(.) with λ_1 =20, $\lambda_2 = 4$ and $\lambda_3 = 1$.

Multi-layer line search algorithm [17–19] to improve the GA performances. In addition, to reduce the computational time required by the optimization process, we have designed a parallel version of this method [2]. A particular Matlab implementation of this optimisation method, called Global Optimisation Platform, has been used during this work to obtain the results presented in Section 3.2. It can be downloaded at: `http://www.mat.ucm.es/momat/software.htm`

3 Results

3.1 Model Validation

In this section, we present the numerical experiments used to check the ability of the model to reproduce real observations. These experiments, presented in Sections 3.1.1 and 3.1.2, aim to validate the oil concentration evolution predicted by our model when no pumping process is considered.

To accomplish this, we compare the model results with real satellite images of the Prestige and the Oleg Naydenov hazards. Indeed, as done in other similar works (see, e.g., [4]), in case of Eulerian models, images give a reasonable representation of the continuous distribution of the oil spill at a given date and can be compared with the continuous distribution returned by the model. In the case of Lagrangian models, the use of buoys data for model validations seems to be also appropriate (see e.g., [1]).

3.1.1 Prestige Case

On 13 November, 2002, the 'Prestige' ship started to spill oil in the open sea near the Galician coasts, Spain [27]. The authorities decided to send the ship far from the Spanish coasts. The ship sank in the Atlantic Ocean on 19 November 2002. Around 10 million gallons of crude oil were spilled, polluting thousands of kilometres of coastline in Spain, France and Portugal [5]. This spill is considered as the largest environmental disaster in the history of both Spain and Portugal, and the cost of this hazard was evaluated to be more than 770 million euros [20]. We use our mathematical model, without the pumping process, to simulate the oil concentration evolution from the beginning of the Prestige event on 13 November 2002 up to 17 November 2002 (the only available clear satellite image of the situation was taken this day, before the Prestige ship broke up). Considering this time interval, we use the following model parameters [9]:

- The simulation area was taken as $\Omega \subset [-12.5, -7.5] \times [42, 44.5]$ (in the longitude-latitude coordinate system) which is assumed to be large enough to avoid the oil concentration leaving this domain during the considered time interval, and the considered Spanish land is shown in Figure 2.

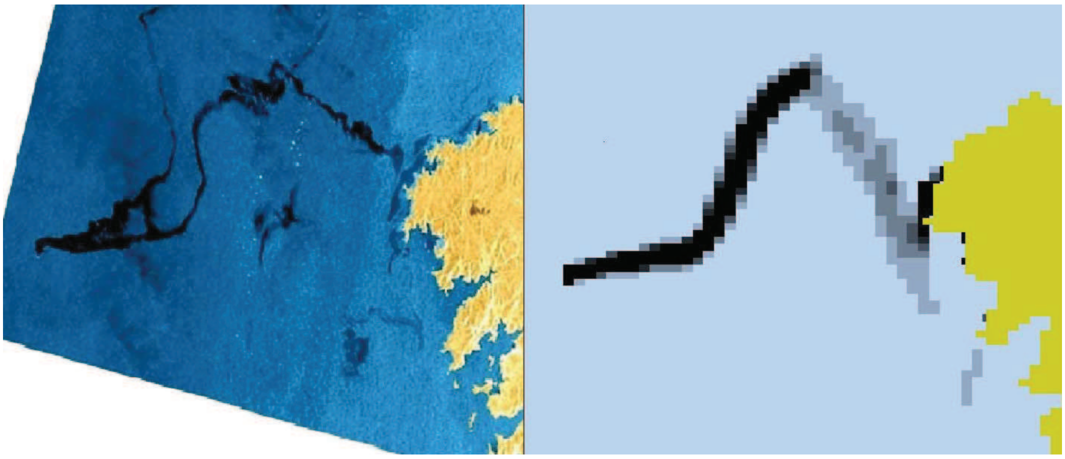

Fig. 2 **(Left)** Satellite image of the Prestige oil spill situation taken by the Envisat ASAR satellite (European Spatial Agency) on 17 November 2002. **(Right)** Oil concentration simulated by the model presented in this work for the same date. The coast is also represented in green.

- The velocity fields of **wind** and **seacurrents** were estimated by considering historical discrete data provided by the research centre Mercator Ocean (Website: `http://www.mercator-ocean.fr`) and completed by using 2D spline interpolation to be able to obtain values at points with no data.
- The trajectory followed by the Prestige ship was taken from the literature [8, 21].
- To our knowledge, the exact amount of oil S spilled by the Prestige ship into the ocean, remains unknown [1, 8, 21]. It is only known that around 54,000 tons of heavy/residual fuel oil were spilled into the sea before the Prestige ship broke on 19 November 2002. So, we have then used the value of $S(t) = 22(kg.s^{-1})$, at every time interval t.
- For the numerical finite volume scheme used to approximate the solution of model presented in Section 2.1, we consider a 100×100 spatial mesh and a time step of 1 hour. All other parameters are given in Reference [16].

Taking into consideration these values, we present in Figure 2 the solution given by our numerical model on 17 November 2002. In the same figure, we also show the satellite image taken by the Envisat ASAR satellite (property of the European Spatial Agency) at the same date (`https://earth.esa.int/web/guest/-/prestige-oil-spill-galicia-spain-1623`). We can observe that graphically both images present similarities regarding the general behaviour of the oil spill shape. This seems to indicate that our model predicts well the evolution of the oil concentration of the Prestige case. However, this figure also illustrates the limitations of our model, which omits to consider some complex physical effects of the sea currents on the oil spill. For instance, our model fails to predict the splitting of the main oil spot in two branches.

3.1.2 Oleg Naydenov Case

We have also validated our method with the case of the Oleg Naydenov hazard in [16]. More precisely, the ship 'Oleg Naydenov' sank near the Canary Islands coasts, Spain, on 14 April 2015. The tanks of this ship were filled with around 1400 tons of oil. During several weeks, this oil spill provoked the pollution of the 'Gran Canaria' Island with several oil spots reaching its coastline. Taking into consideration this case, we present in Figure 3 the solution given by our numerical model on 12 April 2015 and the satellite image taken by a NASA satellite on the same date (http://www.nasa.gov/topics/earth/features/oilspill/)). In this case, there was not other real data available at the time of the forecast. Again, we can observe that both images present similarities regarding the main behaviour of the oil spill shape.

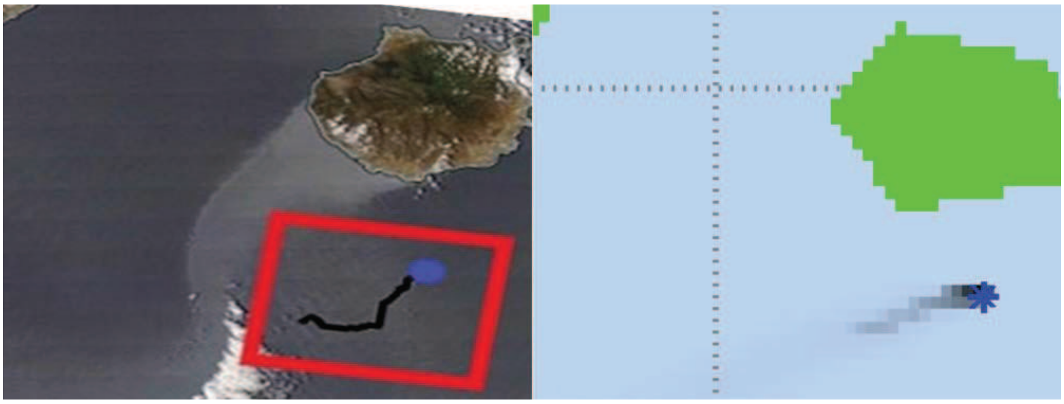

Fig. 3 **(Left)** NASA satellite image presenting the Oleg Naydenov oil spill situation on 21 April 2015. The zone of interest is inside the red rectangle. The ship position is represented by a blue circle and the oil spill with a black line. **(Right)** Oil concentration simulated by the model presented in this work at the same date, considering the computational domain Ω_z. The land is represented in green and the position of the Oleg Naydenov ship by a blue star.

3.2 Skimmer Ship Trajectory Optimization

We are now interested in applying the optimisation method presented in this paper to solve several skimmer ship optimal trajectory problems by considering, as a study case, wind and sea currents data from the Prestige hazard. These problems are designed to study the efficiency of the optimal trajectories considering the objective function formulations (3) or (4) and several values for the power of the pump. Our main objective here is to show the advantage of using optimal trajectories for the cleaning ship. We note that this methodology can be applied for the design of any other cleaning method based on trajectory planning.

3.2.1 Cleaning Scenarios for Different Pumping Power Ships

We study the Prestige hazard with the model parameters presented in Section 3.1.1. However, the model is now run from 13 November 2002 up to 19 November 2002 (i.e., the date when the Prestige ship broke up). The distribution of oil in the open sea on 19 November 2002 simulated by the model (without cleaning process) and the trajectory followed by the Prestige ship are presented in Figure 4. Furthermore, in the same figure, we also give a 3D representation of the oil concentration, in order to better visualise the distribution of oil contamination in Ω. For this reason, from now on, each time the oil concentration is shown, the 3D representation is also displayed.

Now, we activate the pumping process by considering three levels of pumping power Q=0.3 (m s^{-1}), 4 (m s^{-1}) and 8 (m s^{-1}). More precisely:

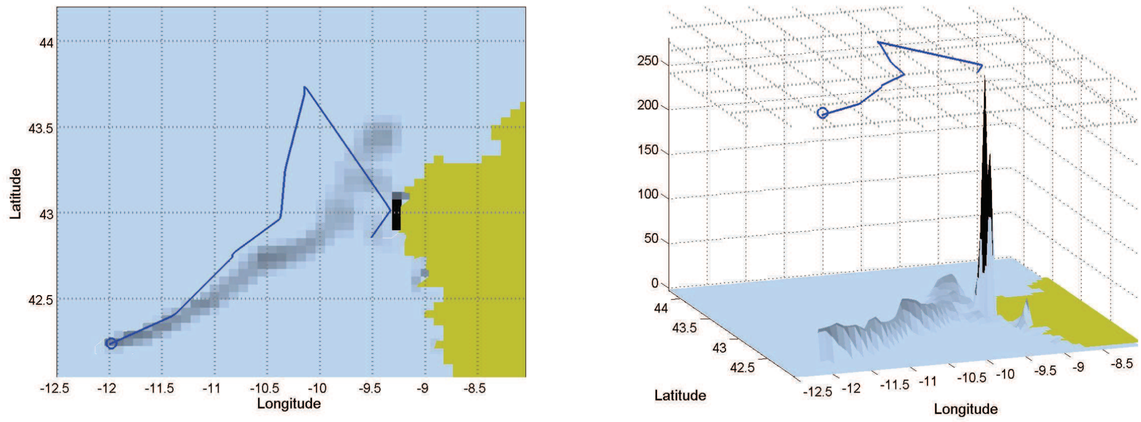

Fig. 4 **(Left)** Top view and **(Right)** 3D view of the final oil concentration distribution on 19 November 2002. Furthermore, the trajectory of the Prestige ship (continuous line) and the final position of the Prestige ship (o) are also presented.

- This first value of $Q = 0.3$ corresponds to the 'Controlled Floating Skimmer' system, build by the Novetec group (Website: `http://novetec.es/body_skimmer.htm`). This device has the advantage of allowing the skimmer ship to pump oil in movement.

- The highest value of $Q = 8$ is similar to the global pumping capacity used by the biggest skimmer ship available at this date: the A-whale (Website: `http://www.marketwatch.com/story/bp-tests-taiwan`

  Although the global pumping system is one of the most powerful, due to technical restrictions this ship cannot perform pumping in movement. Furthermore, it has only been used once during the Gulf of Mexico Deepwater Horizon oil spill disaster in 2010 and was proven inefficient (see: `http://af.reuters.com/article/energyOilNews/idAFN1614683620100716`). However, here we consider such a powerful system by assuming that it can perform the cleaning task in movement.

- Finally, the value of $Q = 4$ is considered in order to study an intermediate pumping power between the A-Whale and the Controlled Floating Skimmer system.

In all these cases, we assume that the pumps are working in ideal conditions, as we omit the decrease in the pumping efficiency due to the type of oil and its physical transformation (e.g., emulsification).

For each value of the pumping power Q, we solve the numerical trajectory Problem (2) using both formulations of the objective function (3) and (4).

The skimmer ship trajectory starts from the position (-9.4, 42.75) (longitude, latitude in degrees) and is parameterised by $N = 5$ interpolation points (obtained by using the optimization method) with a maximum ship velocity of 10 (km.h^{-1}) [13]. To simplify notations, these experiments are denoted by **OPT-Q-F**, where **Q** is replaced by the value of parameter Q and **F** by the type of objective function used.

In order to study the advantage of the optimised results obtained here, we compare the objective function values obtained with the computed optimal trajectories using the straightforward trajectory that simply follows the Prestige ship (this trajectory seems to be the first intuitive option taken by the authorities in the case of oil spill accidents). We make this comparison using different values of the pumping power Q and starting the trajectory from position (-9.4, 42.75), reaching the Prestige ship (at speed $V_{\max}$) and then following exactly the Prestige ship. These experiments are denoted by **PT-Q-**(3) and **PT-Q-**(4), according to the objective function formulation (notation **PT** means following the Prestige Trajectory).

3.2.2 Results for Considered Cleaning Scenarios

We first present and analyse the results obtained when considering the objective function formulation (3), which aims to reduce the amount of oil over the whole area. In this case, the considered experiments are **OPT-0.3-**(3), **OPT-4-**(3), **OPT-8-**(3), **PT-0.3-**(3), **PT-4-**(3) and **PT-8-**(3). We recall that, without pumping the final amount of spilled oil on 19th November 2002 (i.e., the final value of the objective function considering **PT-0-**(3)) is around 54,000 tons of oil. The obtained optimal trajectory and the final oil concentration distribution are shown in Figures 5 and 6. The final values of the objective function (3) (i.e., the amount (in tons) of oil remaining in the sea at the final date) and the reduction in percentage of this value regarding the scenario without skimmer ship are given in Table 1.

Table 1 Objective function (3) value (**O. Func.**) expressed in tons of oil and the percentage of oil pumped (**Reduc.**) given by the experiments (**Exp.**): **OPT-0.3-**(3), **OPT-4-**(3), **OPT-8-**(3), **PT-0.3-**(3), **PT-4-**(3) and **PT-8-**(3)

Exp.	**OPT-0.3-**(3)	**OPT-4-**(3)	**OPT-8-**(3)
O. Func.	50,915	32,241	31,627
Reduc.	6	40	42
Exp.	**PT-0.3-**(3)	**PT-4-**(3)	**PT-8-**(3)
O. Func.	52,712	36,968	23,574
Reduc.	2	31	56

As we can see in Table 1, for the scenarios associated with pumping powers Q=0.3 and Q=4, the optimised trajectories give better results than following the Prestige ship (**OPT** vs **PT**). We can observe in Figures 5 and 6, that in both cases, the skimmer ship remains close to the coast as, due to the sea and wind currents, a large amount of oil is reaches the coast. On the contrary, in the case of the most powerful pump (i.e., Q=8), the optimised trajectory is less efficient than following directly the Prestige ship. Moreover, regarding the optimized trajectory for this case, we note a similar graphical behaviour than the trajectory of the Prestige ship. This seems to indicate that the optimization process try to reproduce this particular trajectory. However, owing to the reduced number of interpolation points (optimisation variables), there exists some discrepancy between both trajectories, which explains the differences observed in the final objective function values. All these results tend to show that, up to a certain pumping power, following the source of contamination is not the best option. An optimisation process should be used in order to analyse which trajectory should be preferred. Another indication that can be derived from these experiments is that the efficiency of the cleaning process is not linearly proportional to the pumping power. Indeed, with $Q = 4$ we found a result almost as efficient as for Q=8. We can deduce that instead of using one powerful skimmer system, various systems with lower power should be preferred. This conclusion is similar to what was observed during the Gulf of Mexico Deep water Horizon oil spill disaster in 2010, where the A-Whale skimmer ship was used but was experimentally demonstrated less efficient (due to restrictions in its movements and difficulties to control its pumping process) than other less powerful skimmer ships (see: `http://af.reuters.com/article/energyOilNews/idAFN1614683620100716`).

We now focus on the results obtained with the formulation (4), that is cleaning the coast, and the experiments **OPT-0.3-**(4), **OPT-4-**(4) and **OPT-8-**(4) versus following the Prestige trajectory **PT-0.3-**(4), **PT-4-**(4) and **PT-8-**(4). In this case, the weighted final amount of spilled oil (or the final value of the objective function considering OPT-0-(4)) was approximately 2.413e+10. The optimal trajectories found at the end of these experiments and the distribution $c_w(x) = \int_0^T \mathrm{coef}(x)c(\tau,x)\mathrm{d}\tau$, are shown in Figures 7 and 8. $c_w(x)$ is a parameter that measures the weighted concentration which have been at point x through the time interval $[0,T]$. The final values of the objective function (4) and the reduction in percentage of this value with respect to the scenario without pumping are given in Table 2. In addition, we also present the final oil concentration distribution c in Figures 9 and 10.

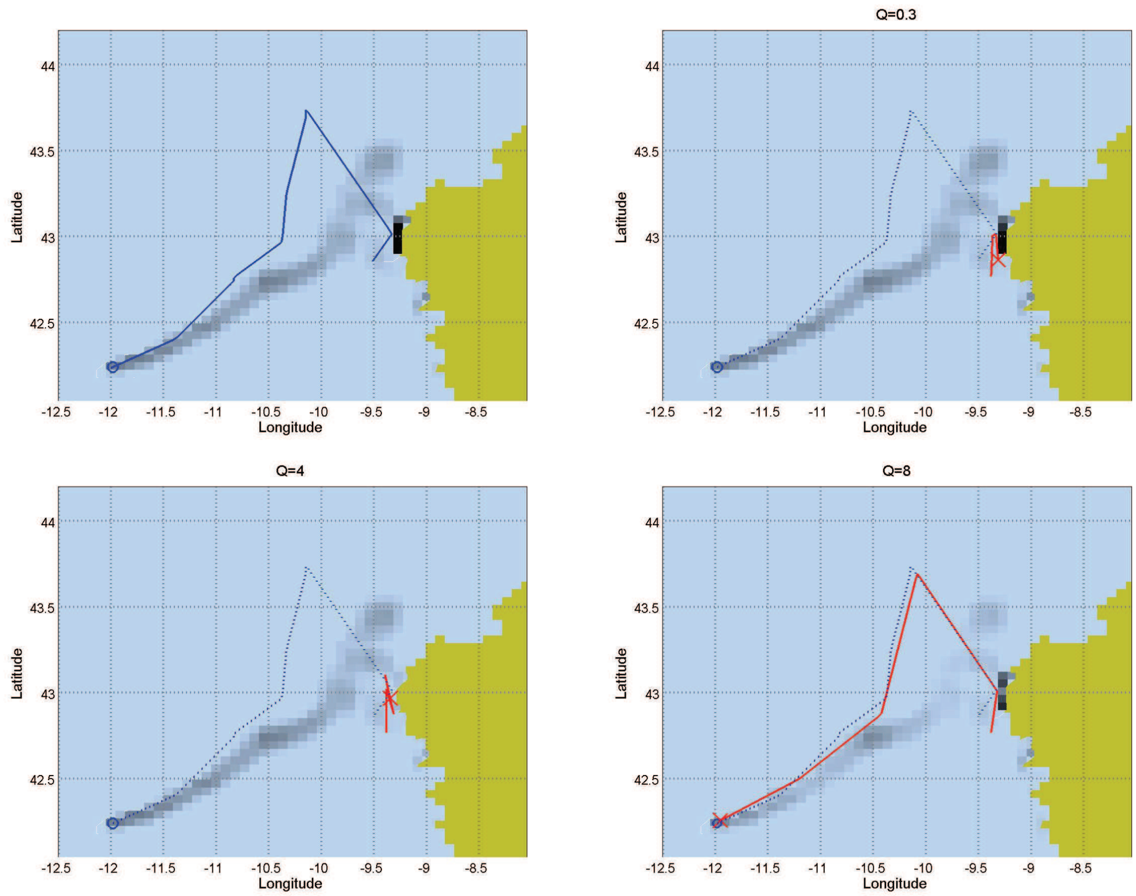

Fig. 5 Top view of the final oil concentration distribution at 19 November 2002, skimmer ship trajectory (continuous red line), final position of the skimmer ship (x) and final position of the Prestige ship (o) for the experiments: (**Top-Left**) trajectory of the Prestige ship (continuous blue line) with no pumping process, (**Top-Right**) **OPT-0.3-**(3), (**Bottom-Left**) **OPT-4-**(3) and (**Bottom Right**) **OPT-8-**(3). The trajectory of the Prestige ship is presented in dotted blue line.

Finally, the final values of the objective function (3) and the reduction in percentage of this value with respect to the scenario without pumping are given in Table 3.

Table 2 Objective function (4) value (**O. Func.**) and percentage reduction (**Reduc.**) of this value regarding the scenario Q=0 given by the experiments (**Exp.**): **OPT-0.3-**(4), **OPT-4-**(4), **OPT-8-**(4), **PT-0.3-**(4), **PT-4-**(4) and **PT-8-**(4).

Exp.	**OPT-0.3-**(4)	**OPT-4-**(4)	**OPT-8-**(4)
O. Func.	2.144e10	1.366e10	1.105e10
Reduc.	11	43	55
Exp.	**PT-0.3-**(4)	**PT-4-**(4)	**PT-8-**(4)
O. Func.	2.3632e10	2.2057e10	1.330e+10
Reduc.	2	9	45

As we can observe in Figures 7 and 8, in all cases, the optimized trajectories remain near the coast, which was expected due to the definition of the cost function (4). Regarding the final values of the objective functions presented in Table 3, we see that all optimised trajectories give better results (i.e, lower objective function values)

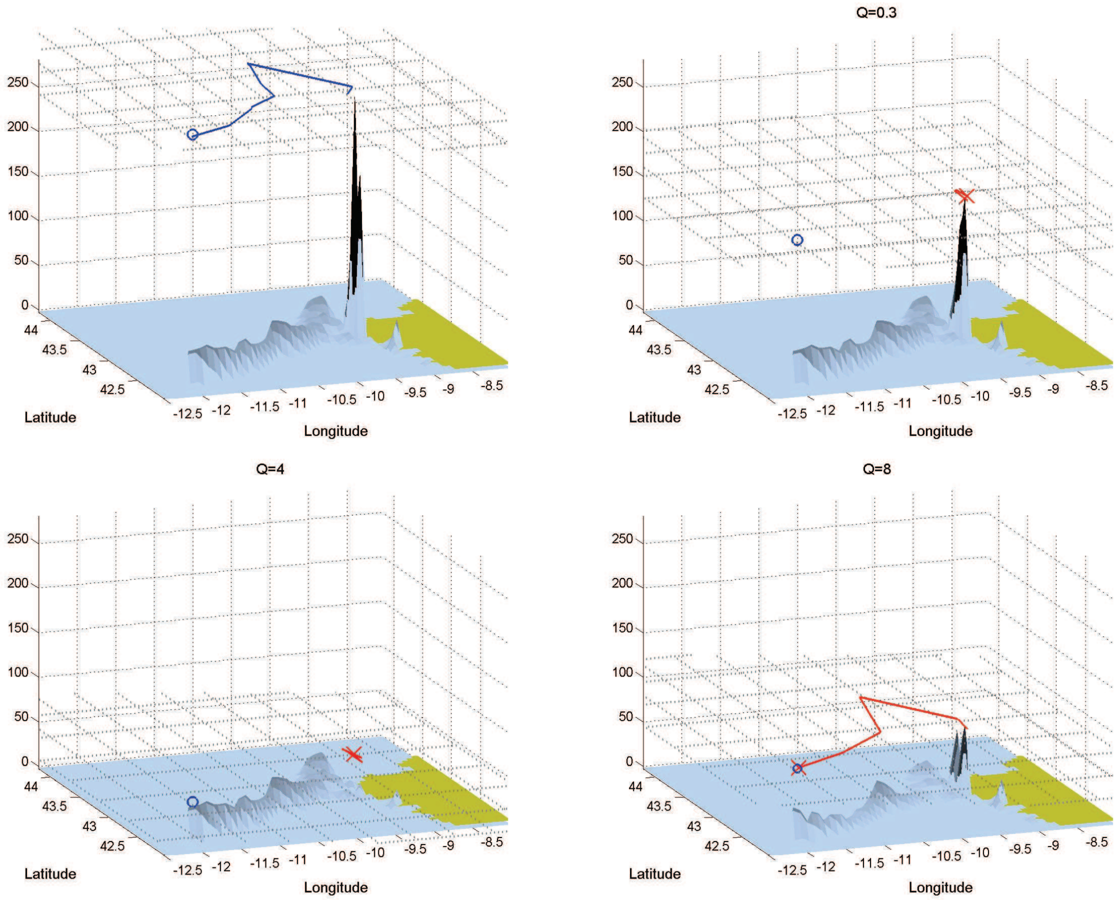

Fig. 6 3D view of the final oil concentration distribution on the 19th of November 2002 for the experiments: (**Top-Left**) case with no pumping process, (**Top-Right**) **OPT-0.3-**(3), (**Bottom-Left**) **OPT-4-**(3) and (**Bottom Right**) **OPT-8-**(3). A plane at the same height as the maximum value of the oil concentration is also presented. In this plane the skimmer ship trajectory (continuous red line), the Prestige ship trajectory when there is no pumping process (continuous blue line), final position of the skimmer ship (x) and final position of the Prestige ship (o) are depicted.

than the trajectory following the Prestige ship. Even in the scenario of using the most powerful pump Q=8, when following the Prestige ship, an important amount of contamination reaches the coast. This seems to indicate that in the cases when protecting the coast is the objective, the best strategy is to concentrate the cleaning effort around the coast. Regarding the amount of remaining oil in the sea reported in Table 3, we see, as expected, that these values are worst than considering the optimization process with formulation (3).

Focusing on the final oil concentration depicted in Figures 9 and 10, we observe that the contamination has been reduced near the coast but remains almost unchanged in the open sea. Thus, a better option should be to clean both coast and open sea. For instance, we can use a skimmer ship following the Prestige vessel and another ship following the optimal trajectory using objective function (4). In order to illustrate this idea, we consider two skimmer ships with Q =8 (m.s^{-1}), one following the trajectory given by **OPT-8-**(4) and another following the Prestige vessel. In this case, the final amount of oil remaining in the sea is 11,837 tons, which represents a decrease of 88% in the value without pumping. The final oil concentration distribution c is presented on Figure 11, where we can observe the drastic global reduction in oil contamination of the whole domain. This result shows that this last strategy is effective to clean the oil spill.

Table 3 Objective function (4) value (**O. Func.**) expressed in tons of oil and the percent reduction (**Reduc.**) of this value regarding the scenario Q=0 given by the experiments (**Exp.**): **OPT-0.3-**(4), **OPT-4-**(4), **OPT-8-**(4), **PT-0.3-**(4), **PT-4-**(4) and **PT-8-**(4).

Exp.	**OPT-0.3-**(4)	**OPT-4-**(4)	**OPT-8-**(4)
O. Func.	50,973	41,233	40,136
Reduc.	6	24	26
Exp.	**PT-0.3-**(4)	**PT-4-**(4)	**PT-8-**(4)
O. Func.	52,712	36,968	23,574
Reduc.	2	31	56

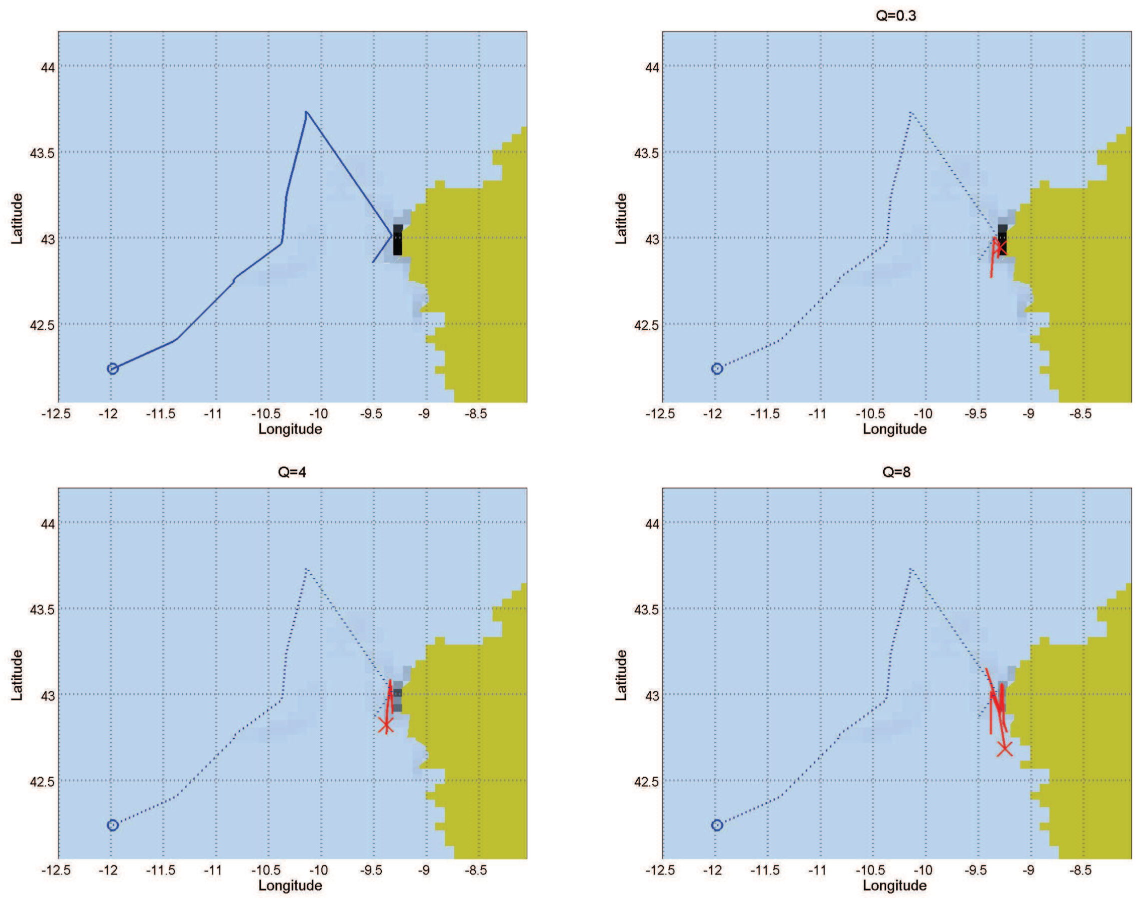

Fig. 7 Top view of the distribution c_w, defined in Section 3.2.2, on 19 2002, skimmer ship trajectory (continuous red line), final position of the skimmer ship (x); final position of the Prestige ship (o) for the experiments: (**Top-Left**) trajectory of the Prestige ship (continuous blue line) with no pumping process, (**Top-Right**) **OPT-0.3-**(4), (**Bottom-Left**) **OPT-4-**(4) and (**Bottom Right**) **OPT-8-**(4). The trajectory of the Prestige ship is also presented in dotted blue line.

4 Discussion

In this article, we have used an original Eulerian mathematical model, discussed in References [2, 13] and [16], to simulate the movement of oil spills in the open sea, taking into account the diffusion, the wind and sea currents, the motion of the contamination source and the effect of a skimmer ship to clean the oil. With

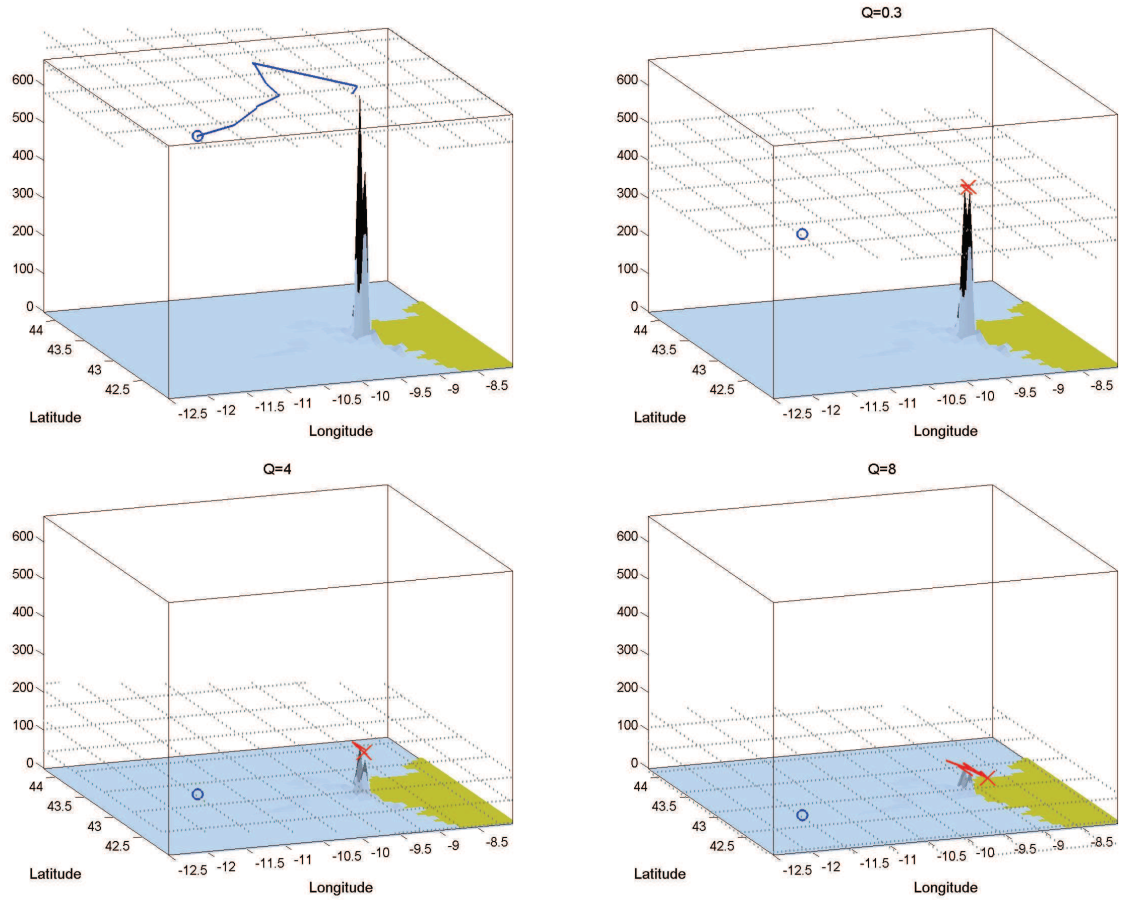

Fig. 8 3D view of the distribution c_w, defined in Section 3.2.2, on 19 November 2002 for the experiments: (**Top-Left**) no pumping process, (**Top-Right**) **OPT-0.3-**(4), (**Bottom-Left**) **OPT-4-**(4) and (**Bottom Right**) **OPT-8-**(4). A plane at the same height as the maximum value of the oil concentration is also presented. In this plane the skimmer ship trajectory (continuous red line), the Prestige ship trajectory with no pumping process (continuous blue line), final position of the skimmer ship (x) and final position of the Prestige ship (o) are depicted.

this model, without considering the pumping process, we were able to approximate the movement of the spill produced by the Prestige vessel in 2002 and that of the Oleg Naydenov in 2016, both in Spain.

Then, we have introduced an optimisation procedure to design optimal trajectories of the considered skimmer ship, improving the amount of pumped oil. Furthermore, we have proposed two different objective functions: one for cleaning the whole domain, and a second formulation that prioritises the coast cleaning. We have used a suitable optimisation algorithm, to find the optimal trajectories for these two different formulations.

To illustrate the importance of our approach, we have solved numerical experiments on a study case created by using some data from the Prestige hazard information. We are aware that the type of oil spilled by the Prestige ship, was not suited for pumping (heavy/residual fuel oil), and, thus, we are not claiming that the results presented here are realistic for this specific scenario. Indeed, the skimmer may deal with light and medium viscosity oil. However, we have used the meteorological data and the trajectory of the ship to create test cases.

We have compared the amount of pumped oil when following the optimal trajectories or when following the Prestige vessel, using three different pumping power alternatives. The results show that when the general formulation of the objective function does not prioritise the coast: (i) for small or medium pumping power, the optimal trajectories remain near the coast anyway (as the highest concentration of oil has gone there because of the effect of the wind and sea currents) and (ii) for high pumping power, the optimal trajectory seems to

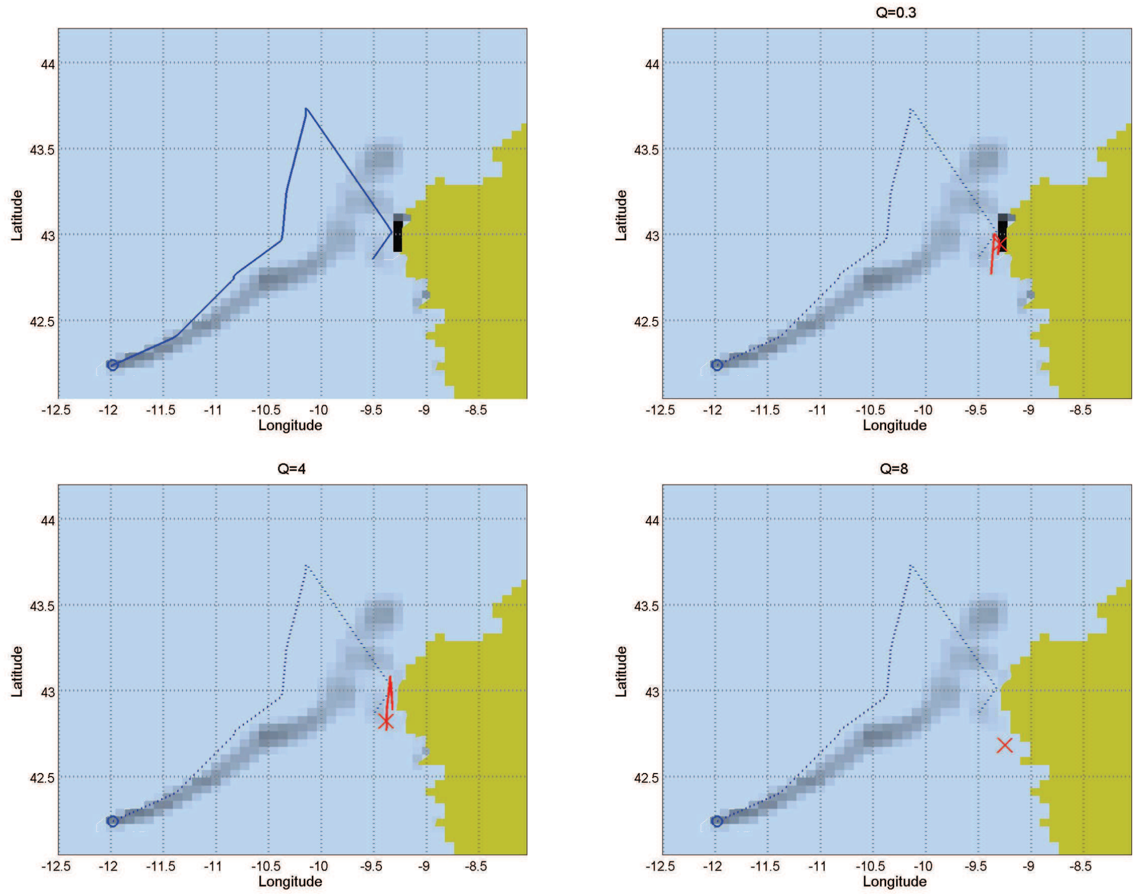

Fig. 9 Top view of the final oil concentration distribution on 19 November 2002, skimmer ship trajectory (continuous red line), final position of the skimmer ship (x) and final position of the Prestige ship (o) for the experiments: (**Top-Left**) trajectory of the Prestige ship (continuous blue line) with no pumping process, (**Top-Right**) **OPT-0.3-**(4), (**Bottom-Left**) **OPT-4-**(4) and (**Bottom Right**) **OPT-8-**(4). The trajectory of the Prestige ship is also presented in dotted blue line.

follow closely the Prestige vessel. This can be explained by the fact that a high pumping power would clean the pollutant as it leaves the vessel.

For the case of the second formulation, independently of the pumping power, the optimal trajectories are much more efficient in cleaning the polluted coast areas than the trajectory that simply follows the polluting ship.

Furthermore, if the option of using two skimmer ships with a high pumping power is available, a good option is to use one skimmer ship near the coast following the optimal trajectory for the function defined in (4), and another one following the polluting source. In this case our results show that we can clean 88 percent of the pollutant oil, in the particular case studied here.

As a final consideration, we insist on the fact that the methodology proposed here is not only limited to skimmer ships, but can also be adapted to any other cleaning devices that require trajectory planning.

In future work, we will improve our model by including additional physical effects on the oil spill evolution, such as emulsification, evaporation or tide currents.

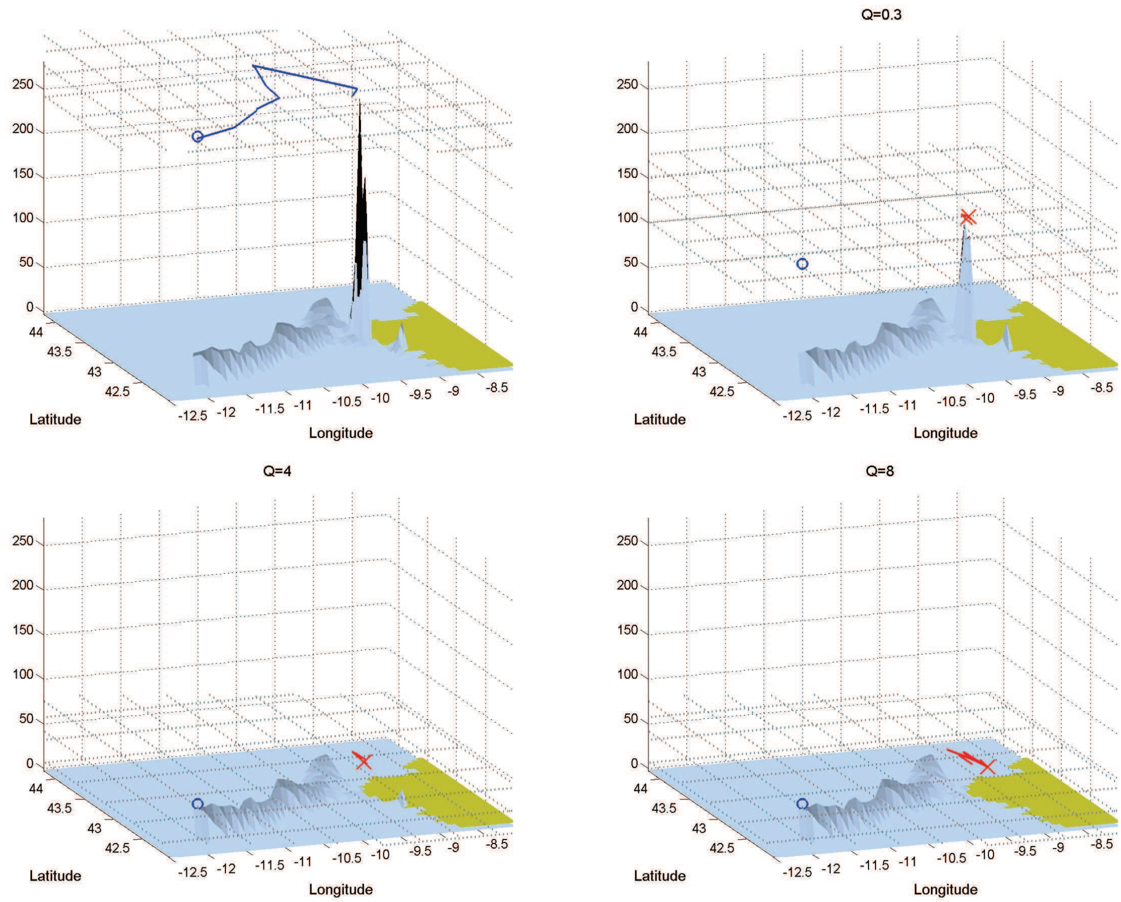

Fig. 10 3D view of the final oil concentration distribution on 19 November 2002 for the experiments: (**Top-Left**) no pumping process, (**Top-Right**) **OPT-0.3-**(4), (**Bottom-Left**) **OPT-4-**(4) and (**Bottom Right**) **OPT-8-**(4). A plane at the same height as the maximum value of the oil concentration is also presented. In this plane the skimmer ship trajectory (continuous red line), the Prestige ship trajectory with no pumping process(continuous blue line), final position of the skimmer ship (x) and final position of the Prestige ship (o) are depicted.

Acknowledgment

This work was carried out thanks to the financial support of the Spanish ‘Ministry of Economy and Competitiveness’ under project MTM2015-64865-P, the research group MOMAT (Ref. 910480) supported by ‘Banco Santander’ and ‘Universidad Complutense de Madrid’, the ‘Junta de Andalucía’ and the European Regional Development Fund through project P12-TIC301, the ‘European Space Agency’ through project 14161, the Institute of Applied Mathematics at the National University of México Proyecto PAPIIT IT100616 UNAM, the research centre ‘Mercator Ocean’ through project 2012_130/NCUTD/59 and the Spanish ‘Agencia Estatal de Meteorología’ through project 990130301 for carrying out this work. We would also like to thank the Spanish agency ‘Puerto de Estados’ and the company ‘Novetec’ for the valuable help provided during this work.

References

[1] A.J. Abascal, S. Castanedo, F.J. Mendez, R. Medina, and I.J. Losada, Calibration of a Lagrangian Transport Model Using Drifting Buoys Deployed during the Prestige Oil Spill, Journal of Coastal Research, 251: 80-90, 2009.
[2] C. Alavani, R. Glowinski, S. Gomez, B. Ivorra, P. Joshi, A.M. Ramos, Modelling and simulation of a polluted water

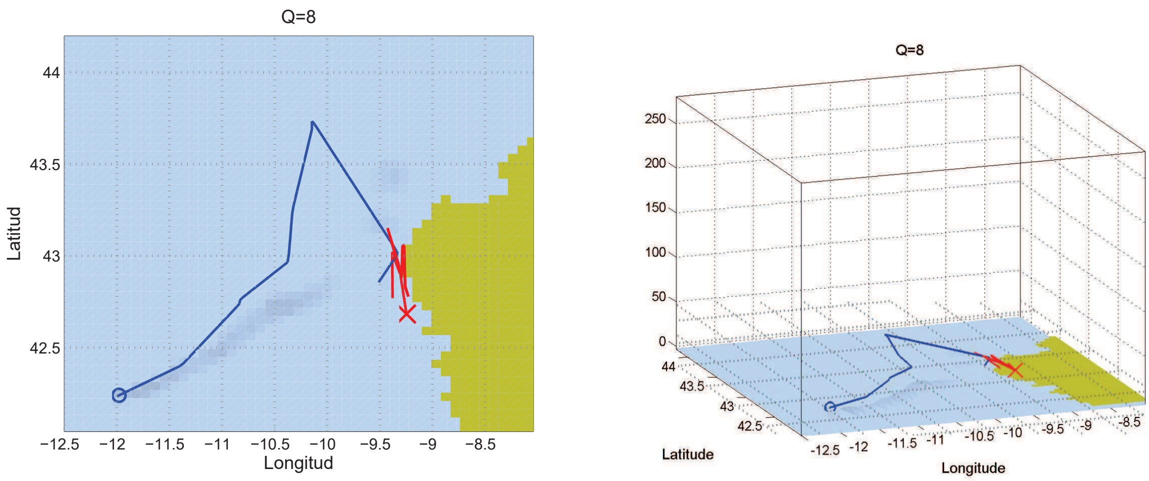

Fig. 11 **(Left)** Top view and **(Right)** 3D view of the final oil concentration distribution on 19 November 2002, skimmer ship trajectory (continuous line), final position of the skimmer ship (x) and final position of the Prestige ship (o) for the experiments with two skimmer ships, one following the trajectory generated by **OPT-8-**(4) and another one following the Prestige ship trajectory. The trajectory of the prestige ship is also presented in dotted line. In the 3D view case, a plane at the same height as the maximum value of the oil concentration is also presented. In this plane the skimmer ship trajectory (continuous line), Prestige ship trajectory (dotted line), final position of the skimmer ship (x) and final position of the Prestige ship (o) are depicted.

pumping process, Mathematical and Computer Modelling, 51: 461-472, 2010.
[3] AukeVisser, Historical Tankers Site. A-Whale characteristics. Available at: http://www.aukevisser.nl/supertankers/bulkers/id453.htm
[4] A. Azevedo, A. Oliveira, A.B Fortunato, X. Bertin, Application of an Eulerian-Lagrangian oil splill modeling system to the Prestige accident: trajectory analysis Journal of Coastal Research Special Issue 56 : 777-781, 2009.
[5] C.F. Balseiro, P. Carracedo, B. Gómez, P.C. Leitão, P. Montero, L. Naranjo, E. Penabad, V. Pérez-Muñuzuri, Tracking the Prestige oil spill: An operational experience in simulation at MeteoGalicia, Weather, 58(12): 452-458, 2003.
[6] J. Beyer, H. C. Trannum, T. Bakke, P. V. Hodson, T. K. Collier, Environmental effects of the Deepwater Horizon oil spill: A review, Marine Pollution Bulletin, 110 (1): 28–51, 2016.
[7] A.D. Carpenter, R.G. Dragnich, Marine Operations and Logistics During the Exxon Valdez Spill Cleanup, Oil Spill Conference Proceedings, 205-211, 1991.
[8] S. Castanedo, R. Medina, I.J. Losada, C. Vidal, F.J. Mendez, J. Osorio, A. Puente, The Prestige oil spill in Cantabria (Bay of Biscay). Part I: Operational forecasting system for quick response, risk assessment and protection of natural resources, Journal Of Coastal Research, 22(6): 1474-1489, 2006.
[9] P.S. Daling, M.O. Moldestad, The Prestige Oil-Weathering Properties. Marine Environmental Technology. 2: 1-4, 2003.
[10] M. Fingas. The Basics of Oil Spill Cleanup, Second Edition, CRC Press, 2000.
[11] R. Glowinski, P. Neittaanmaki, Partial Differential Equations. Modelling and Numerical Simulation, Series: Computational Methods in Applied Sciences, Springer, 16, 2008.
[12] S. Gomez, G. Fuentes, R. Camacho, M. Vasquez, J. M. Otero, A. Mesejo, N. del Castillo, Application of an Evolutionary Algorithm in well test characterization of Naturally Fractured Vuggy Reservoirs, Society of Petroleum Engineering, SPE No. 103931, 2006.
[13] S. Gomez, B. Ivorra, A.M. Ramos, Optimization of a pumping ship trajectory to clean oil contamination in the open sea, Mathematical and Computer Modelling, 54(1) : 477-489, 2011.
[14] S. Gomez, G. Severino, L. Randazzo, G. Toraldo, J.M. Otero, Identification of the hydraulic conductivity using a global optimization method, Agricultural Water Management, 93(3): 504-510, 2009.
[15] International Tanker Owners Pollution Federation. Use of skimmers in oil pollution response, Technical information paper 5, 2014. URL: http://www.itopf.com/knowledge-resources/documents-guides/document/tip-5-use-of-skimmers-in-oil-pollution-response/
[16] B. Ivorra, S. Gomez, R. Glowinski , A.M. Ramos, Nonlinear Advection-Diffusion-Reaction Phenomena Involved in the Evolution and Pumping of Oil in Open Sea: Modeling, Numerical Simulation and Validation Considering the Prestige and Oleg Naydenov Oil Spill Cases. J Sci Comput, 70(3): 1078–1104, 2017.

[17] B. Ivorra, B. Mohammadi, A. and A. M.Ramos, Optimization strategies in credit portfolio management. *Journal of Global Optimization*, 43(2-3):415-427, 2009.
[18] B. Ivorra, B. Mohammadi, and A.M. Ramos, A multi-layer line search method to improve the initialization of optimization algorithms. *European Journal of Operational Research*, 247(13):711-720, 2015.
[19] B. Ivorra, A.M. Ramos, B. Mohammadi, Semideterministic global optimization method: Application to a control problem of the Burgers equation. *Journal of Optimization Theory and Applications*, 135(3):549–561, 2007.
[20] M.L. Loureiro, A. Ribas, E. López, E. Ojea, Estimated costs and admissible claims linked to the Prestige oil spill. Ecological Economics, 59(1): 48-623, 2006.
[21] P. Montero, J. Blanco, J.M. Cabanas, J. Maneiro, Y. Pazos, A. Moroño, C.F. Balseiro, P. Carracedo, B. Gomez, E. Penabad, V. Perez-Muruzuri, F. Braunschweig, R. Fernades, P.C. Leitao and R. Neves, Oil Spill Monitoring, Forecasting on the Prestige-Nassau accident. In: Proceedings 26th Arctic Marine Oil Spill Program (AMOP) Technical Seminar, 2: 1013-1029,2003.
[22] N.O.A.A., Oil Spill case histories 1967-1991. Summaries of significant U.S. and international spills, Office of response and restoration of the U.S. National Ocean, Report HMRAD, 92-11, 1992.
[23] J. L. S. Pinhol, J. S. Antunes do Carmo and J. M. P. Vieira, Numerical modelling of oil spills in coastal zones. A case study Oil and Hydrocarbon Spills III, CA Brebbia (Editor) 2002.
[24] V. Ramšak, V. Malačič, M. Ličer, J. Kotnik, M. Horvat, D. Žagar, High-resolution pollutant dispersion modelling in contaminated coastal sites, Environmental Research, 125:103-112, 2013.
[25] M. Reed, P. Daling, A. Lewis, M.K. Ditlevsen, B. Brørs, J. Clark, D. Aurand, Modelling of dispersant application to oil spills in shallow coastal waters, Environmental Modelling & Software, 19(7-8): 681-690, 2004.
[26] J.M. Sayol, A. Orfila, G. Simarro, D. Conti, L. Renault, A. Molcard (2014) A Lagrangian model for tracking surface spills and SaR operations in the ocean, Environmental Modelling & Software, 52: 74-82.
[27] S.K. Skinner, W.K. Reilly (2008) The Exxon Valdez Oil Spill. National Response Team.
[28] D. Di Serafino, S. Gomez, L. Milano, F. Riccio and G. Toraldo (2010) A genetic algorithm for a global optimization problem arising in the detection of gravitational waves, Journal of Global Optimization, 48(1): 41-55.
[29] M. L. Spaulding (1988) A state-of-the-art review of oil spill trajectory and fate modeling, Oil and Chemical Pollution 4(1):39-55.
[30] M. L. Spaulding (2017) State of the art review and future directions in oil spill modeling Marine Pollution Bulletin 115(1-2):7–19.
[31] B. Suárez, V. Lopez, B. Pérez-Gómez, N. Aragonés, F. Rodríguez-Artalejo, F. Marqués, A. Guzmán, L.J. Viloria, J.M. Carrasco, J.M. Martín-Moreno, G. López-Abente and M. Pollán (2005) Acute health problems among subjects involved in the cleanup operation following the Prestige oil spill in Asturias and Cantabria (Spain), Environmental Research, 99(3): 413 - 424.
[32] Z. Wang, S.A. Stout (2007) Oil Spill Environmental Forensics: Fingerprinting and Source Identification. Academic Press, Burlington.